OMTN, Volume *17*

Supplemental Information

miR-15a/-16 Inhibit Angiogenesis by Targeting the Tie2 Coding Sequence: Therapeutic Potential of a miR-15a/16 Decoy System in Limb Ischemia

Marie Besnier, Saran Shantikumar, Maryam Anwar, Parul Dixit, Aranzazu Chamorro-Jorganes, Walid Sweaad, Graciela Sala-Newby, Paolo Madeddu, Anita C. Thomas, Lynsey Howard, Sobia Mushtaq, Enrico Petretto, Andrea Caporali, and Costanza Emanueli

Supplementary figure S1

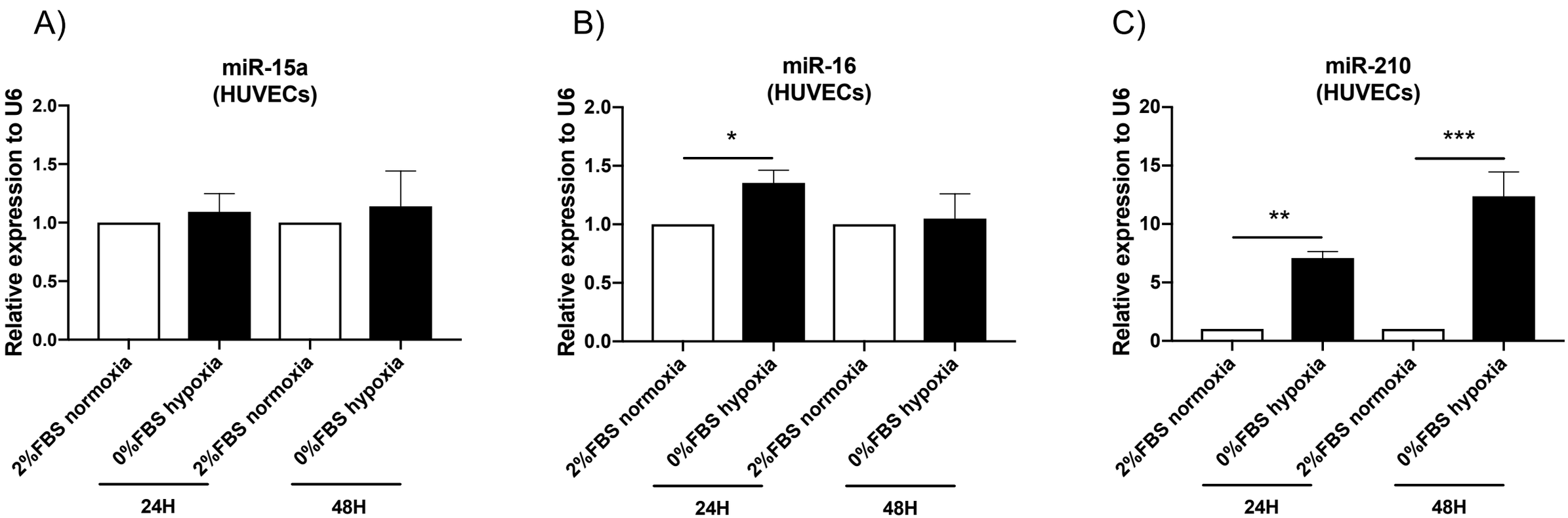

Supplementary figure S2

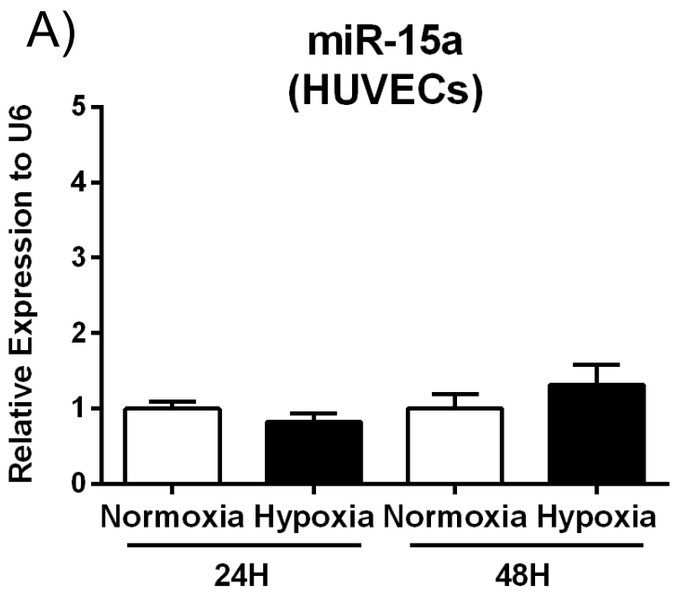

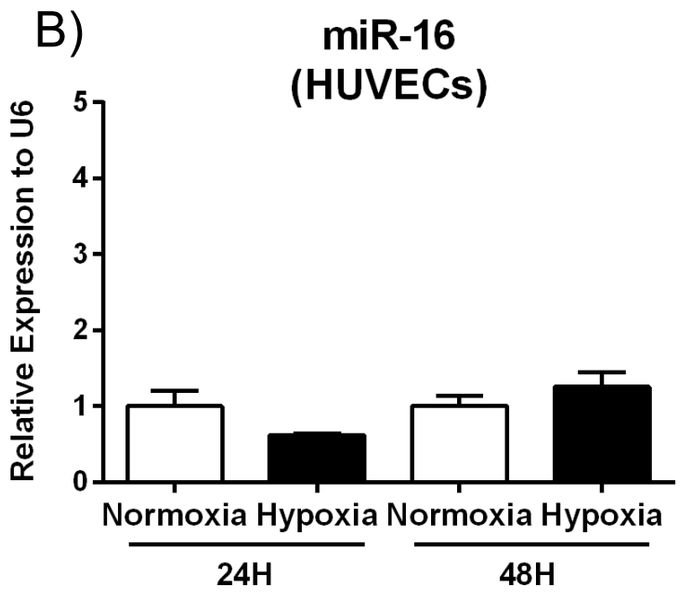

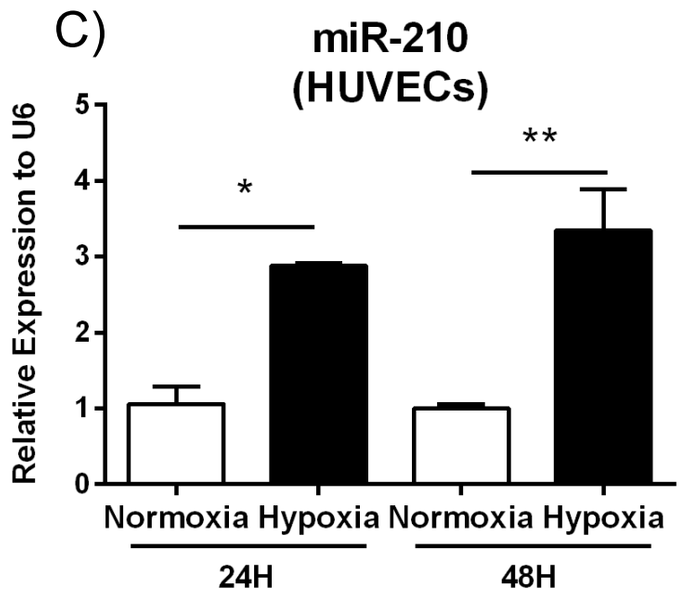

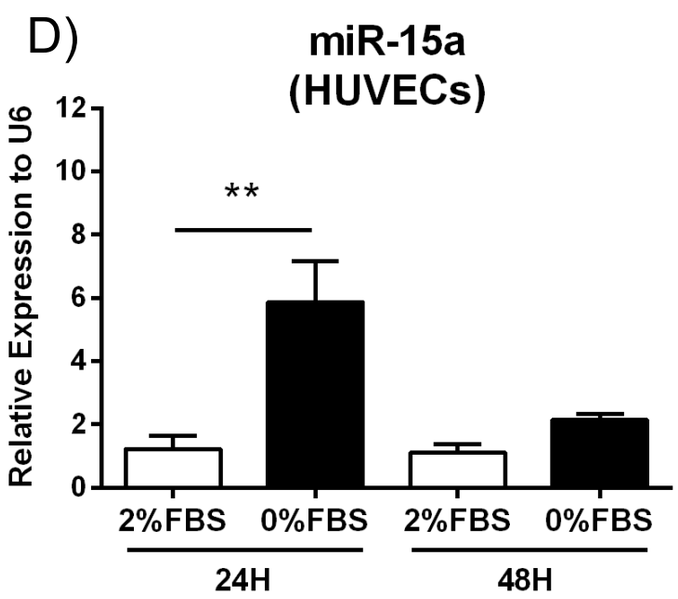

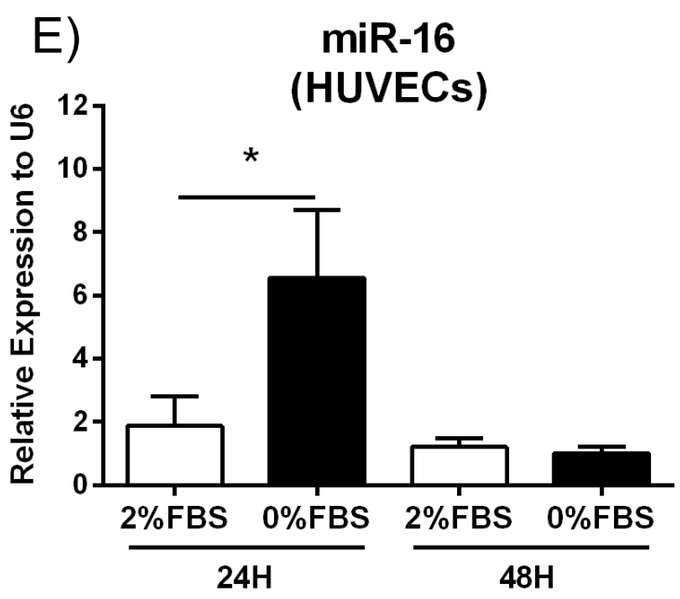

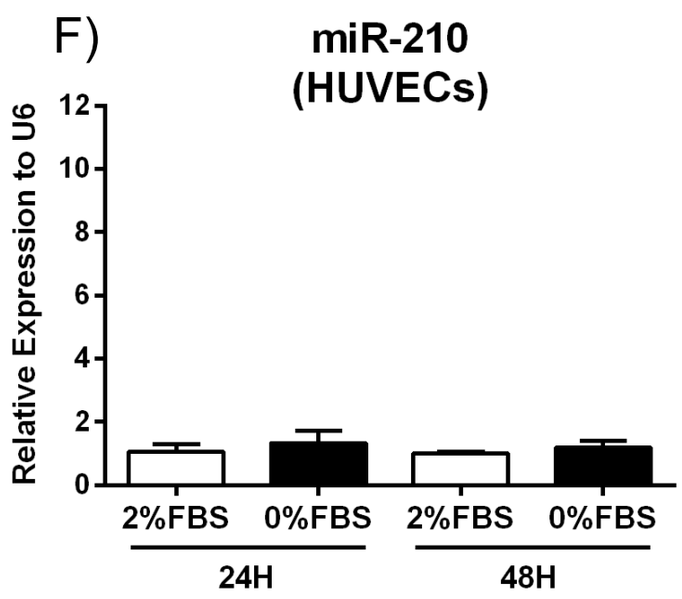

Supplementary figure S3

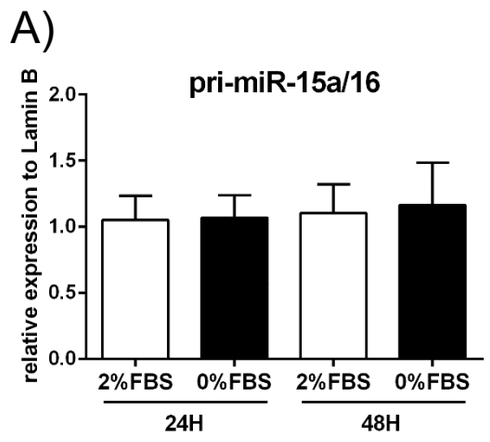

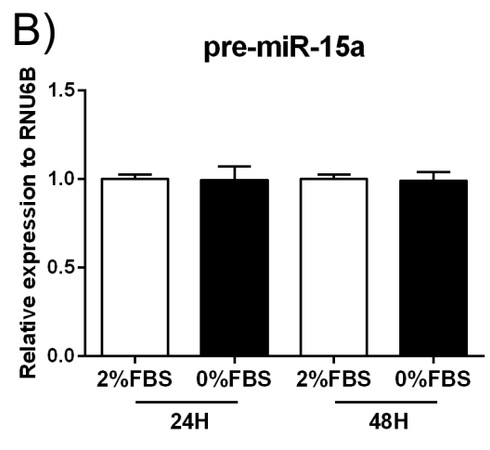

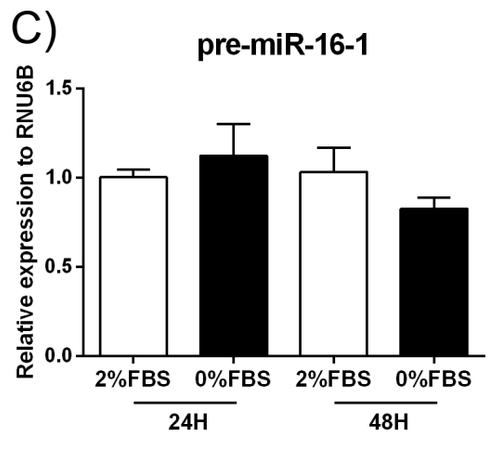

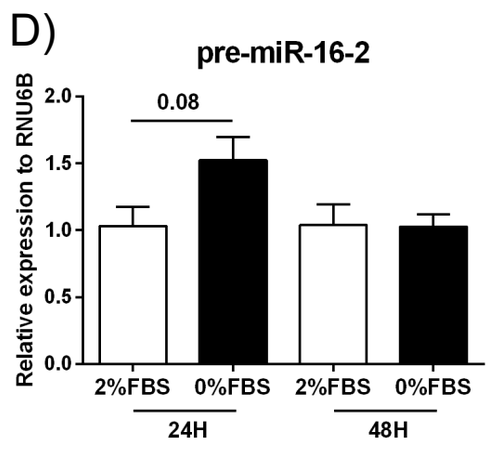

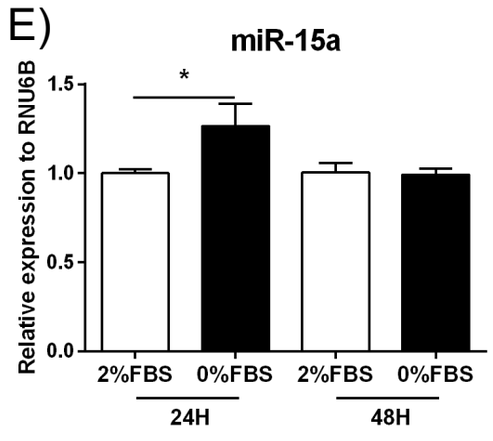

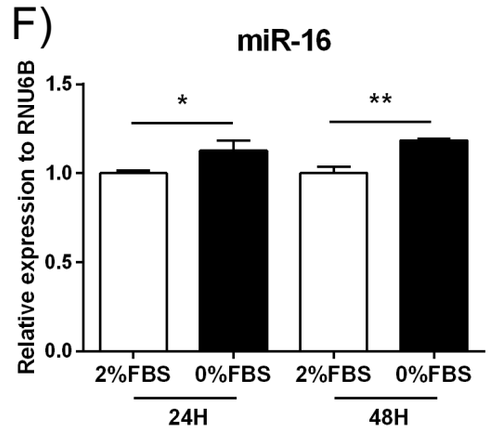

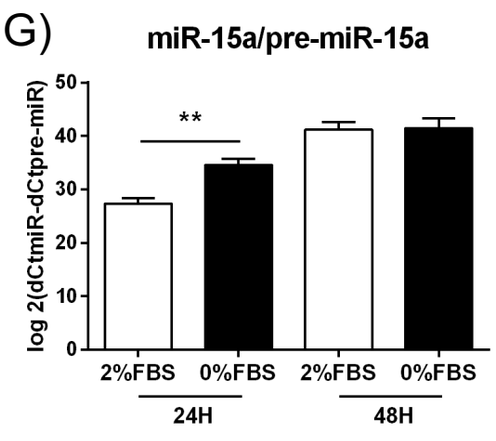

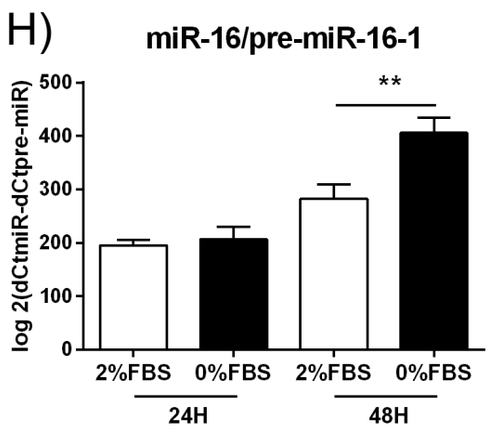

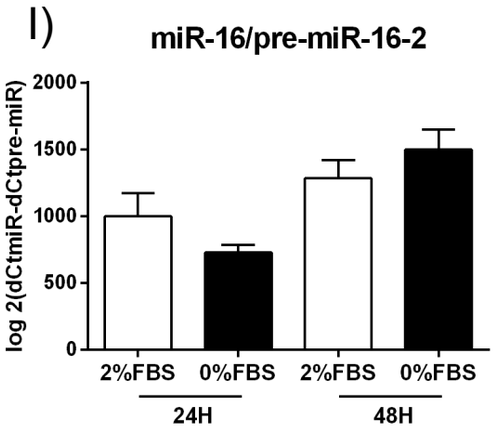

Supplementary figure S4

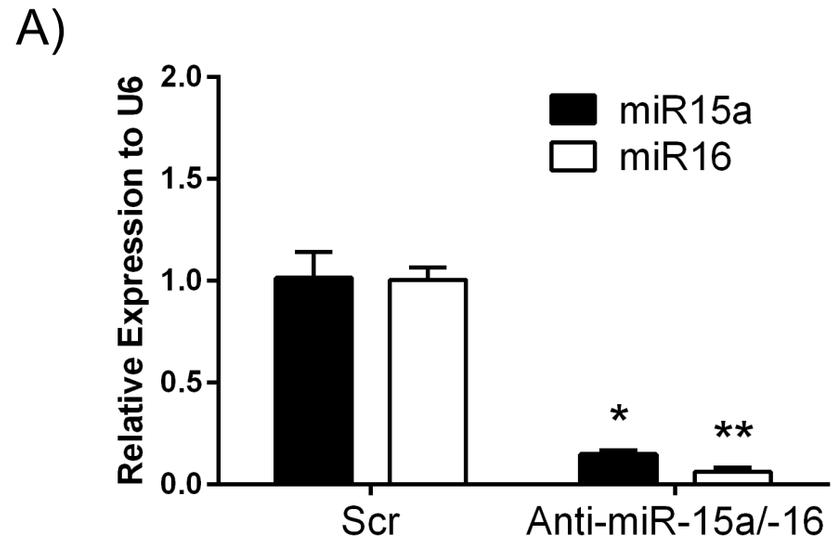

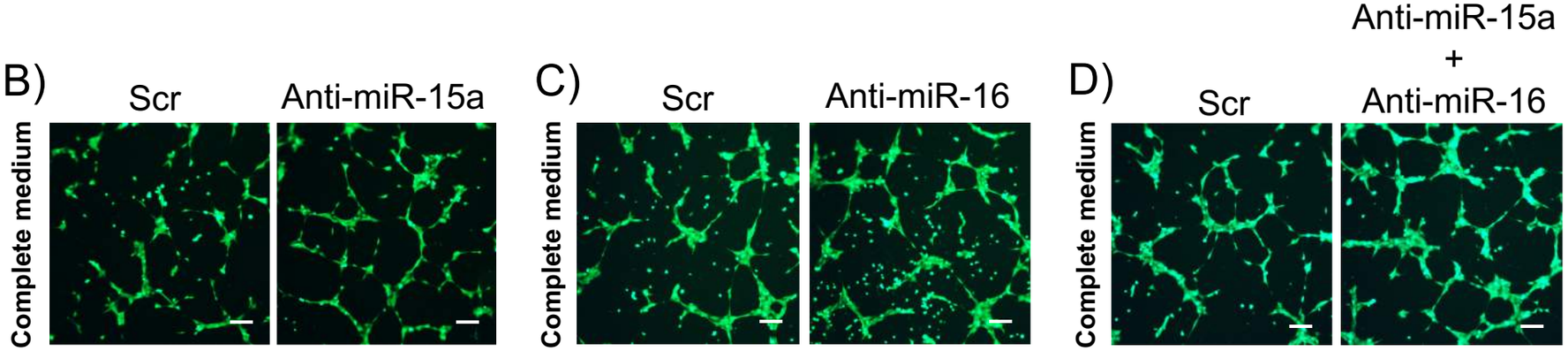

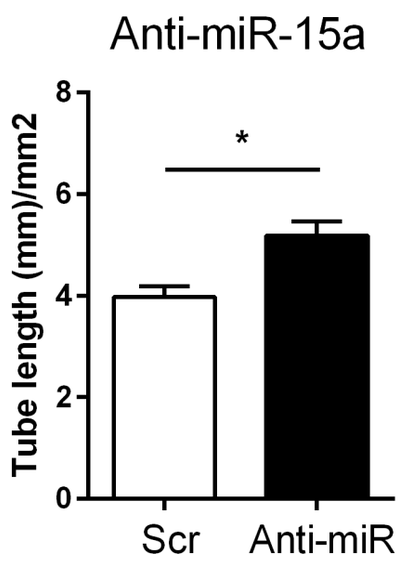

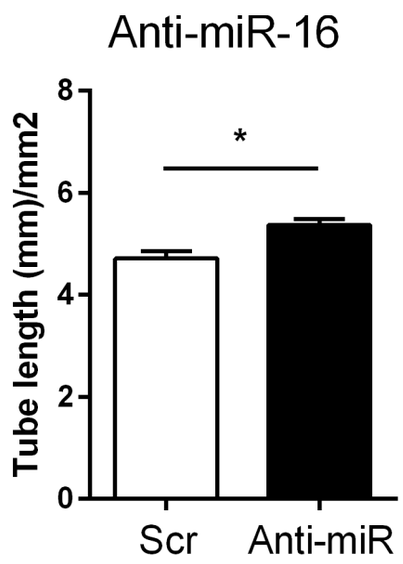

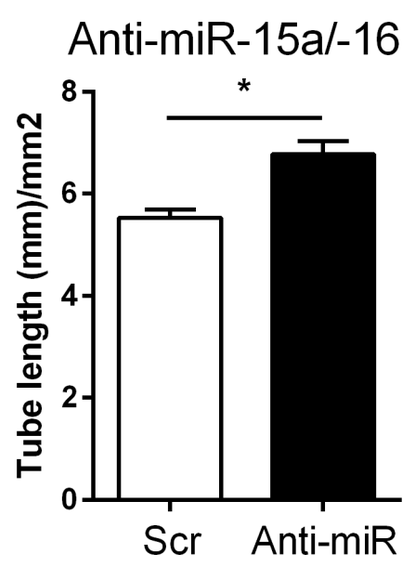

Supplementary figure S5

A)

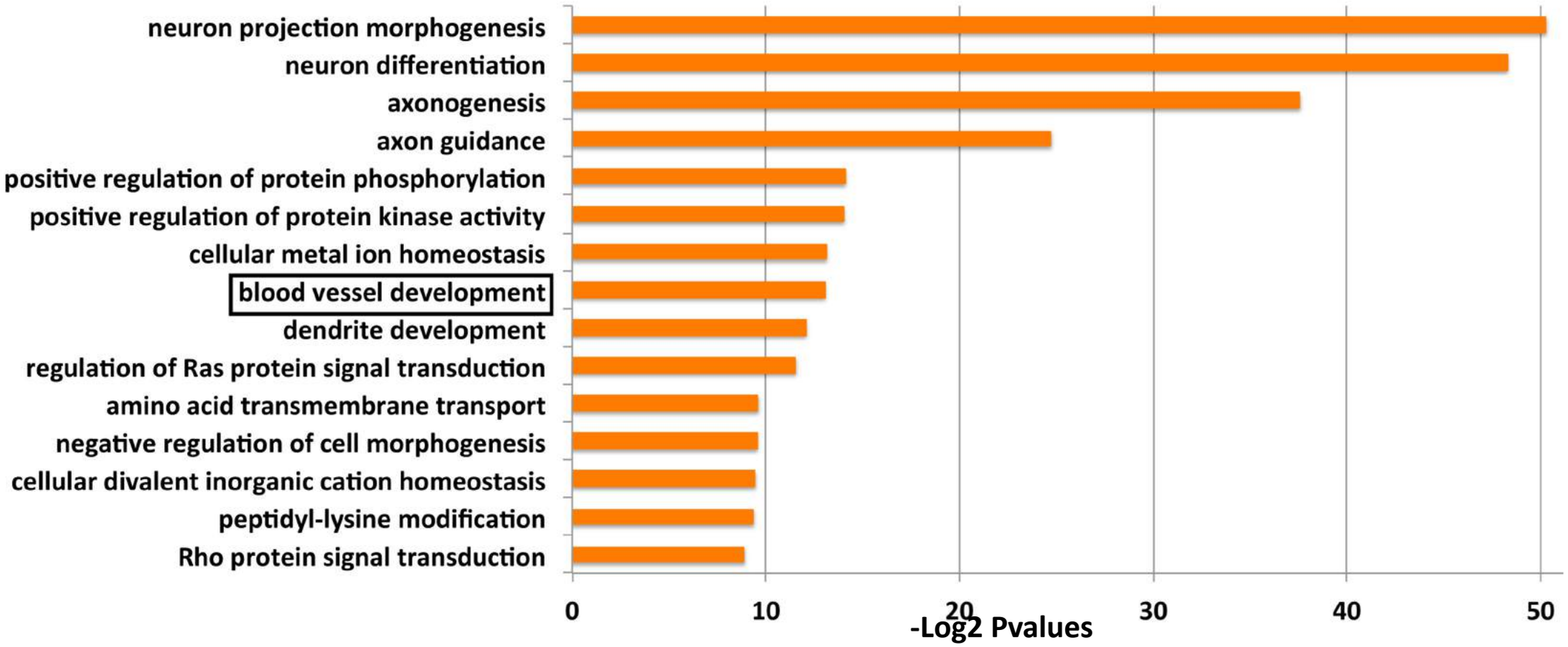

B)

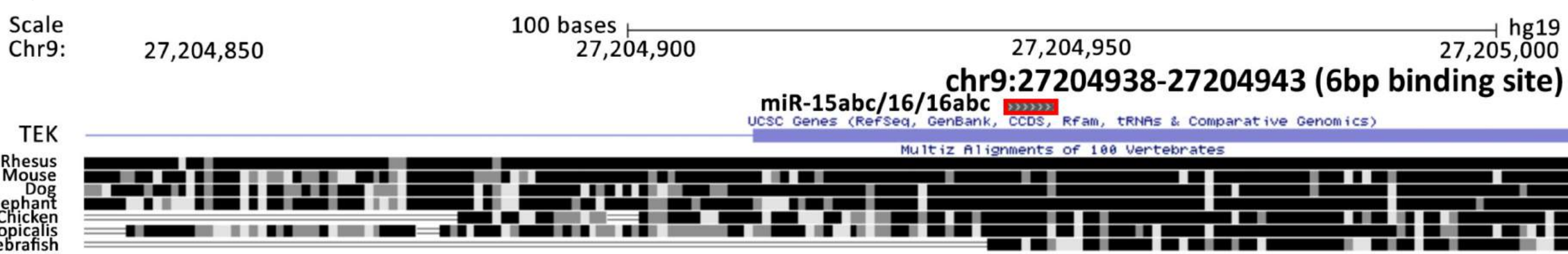

C)

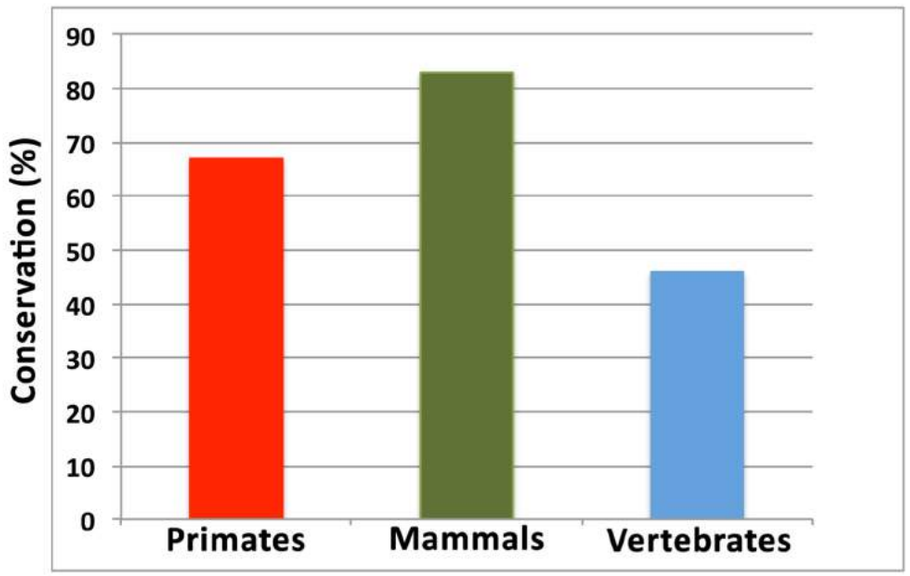

Supplementary figure S6

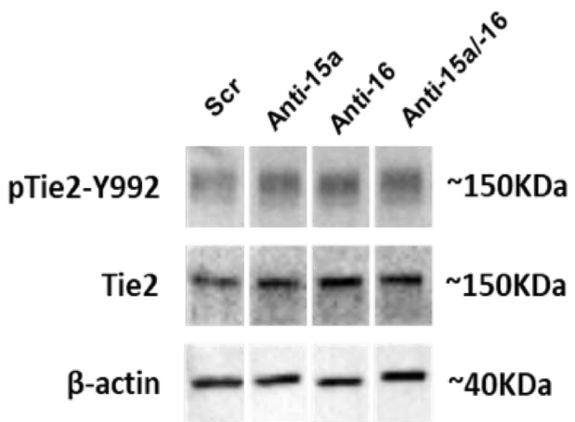

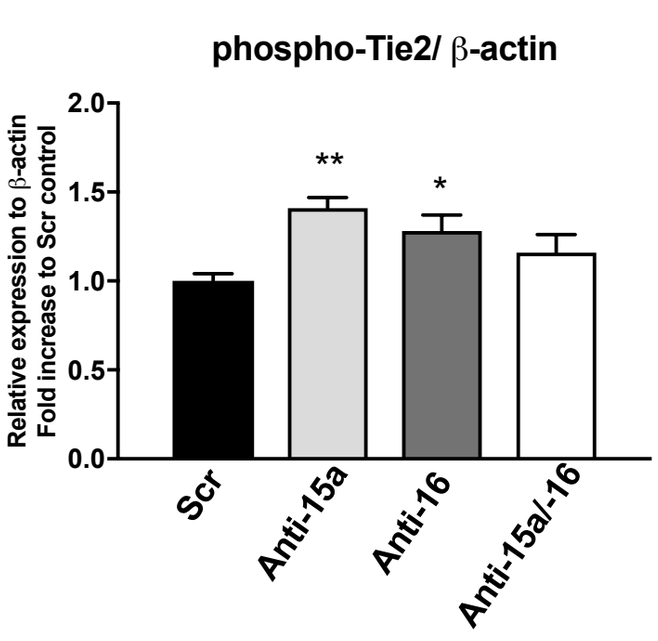

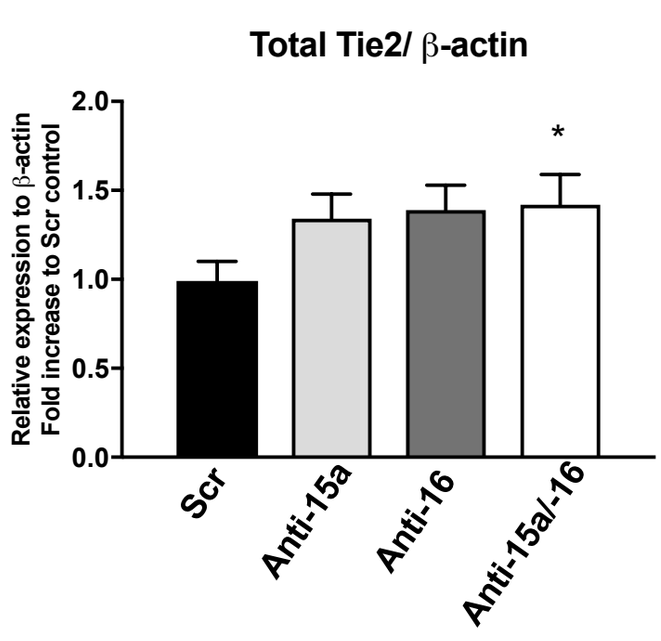

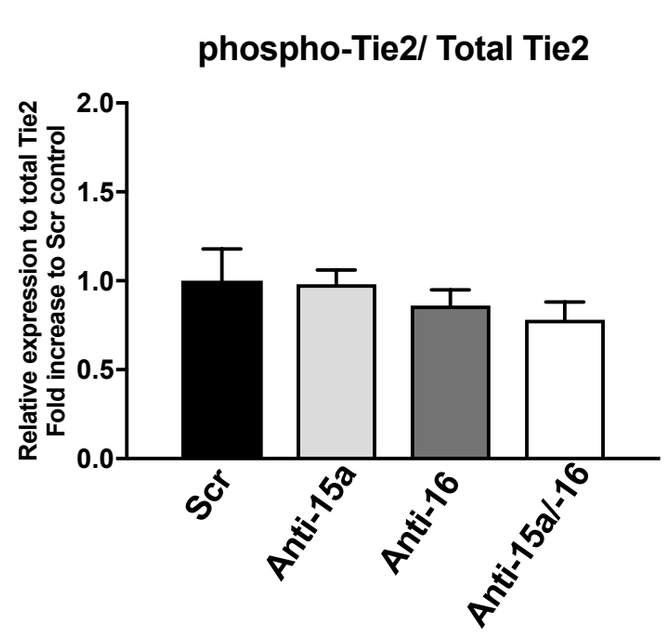

Supplementary figure S7

A)

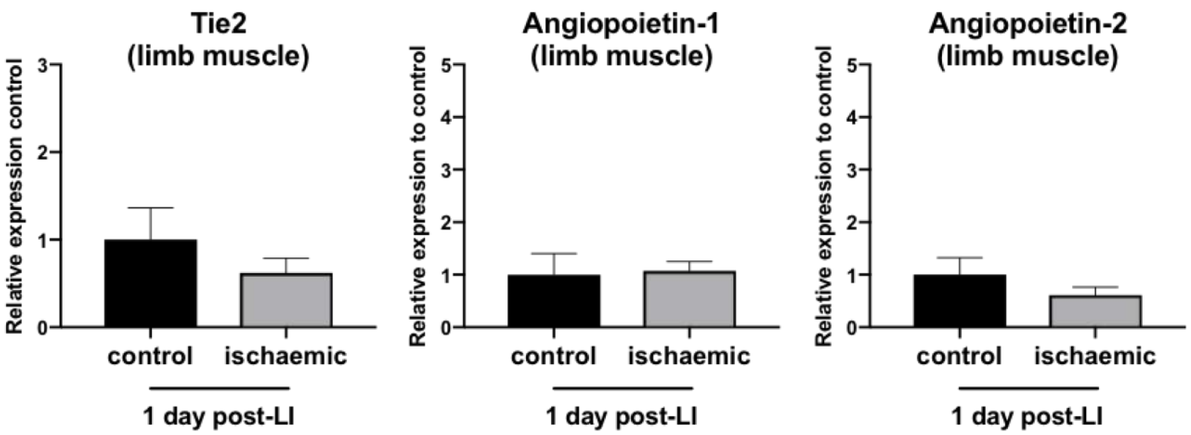

B)

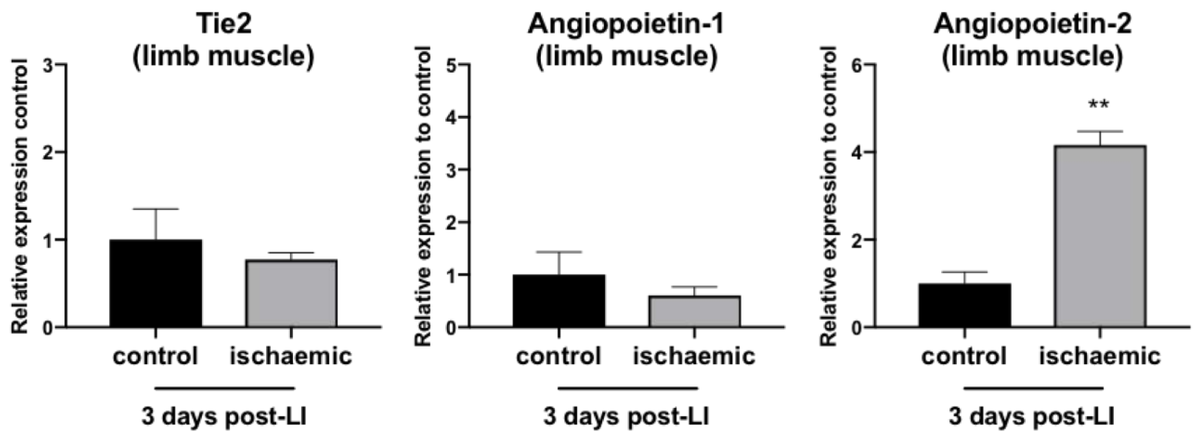

C)

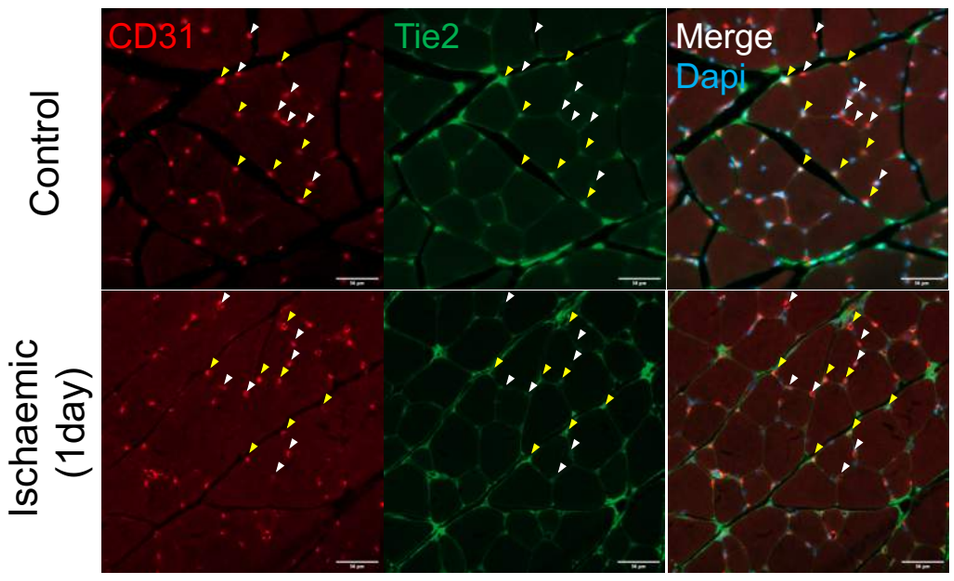

F)

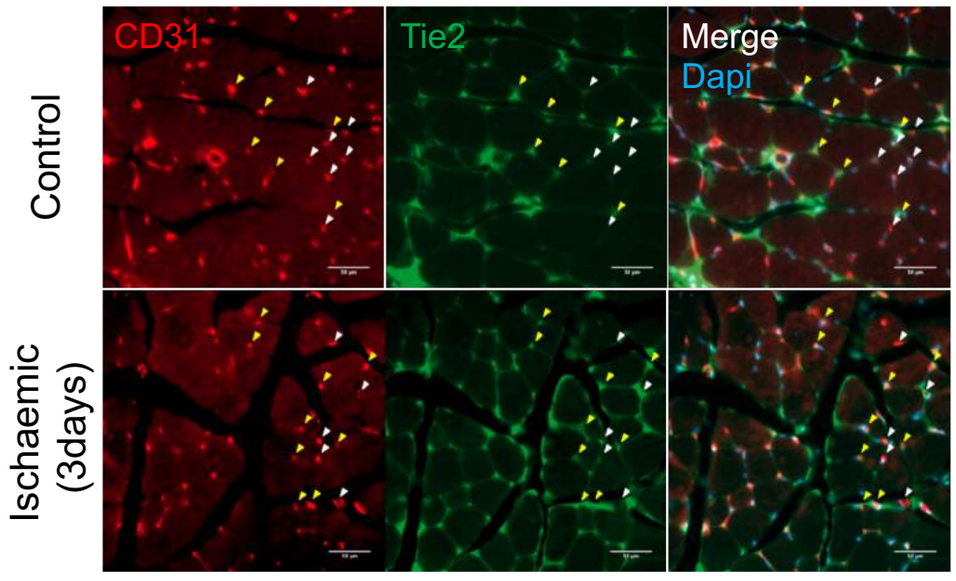

D)

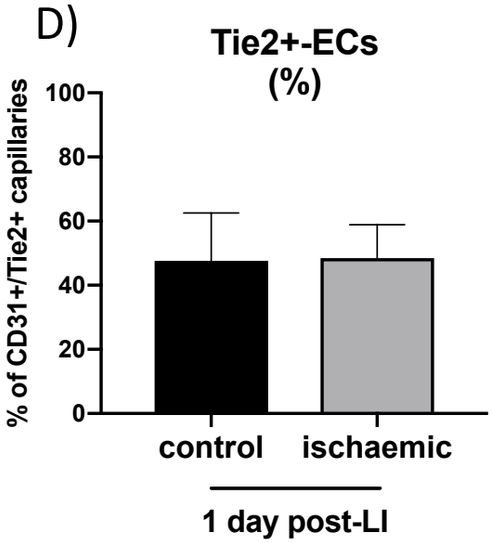

E)

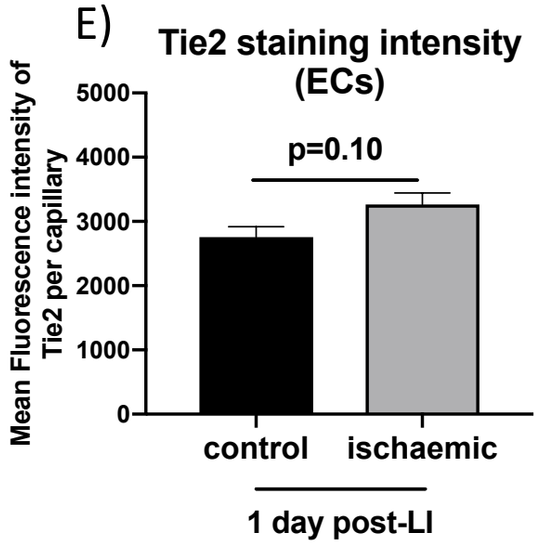

G)

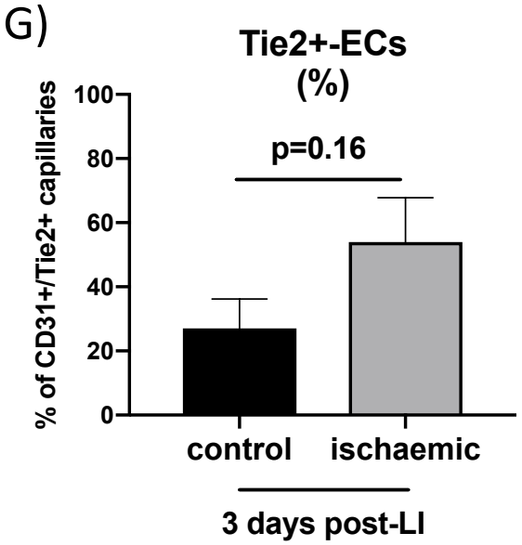

H)

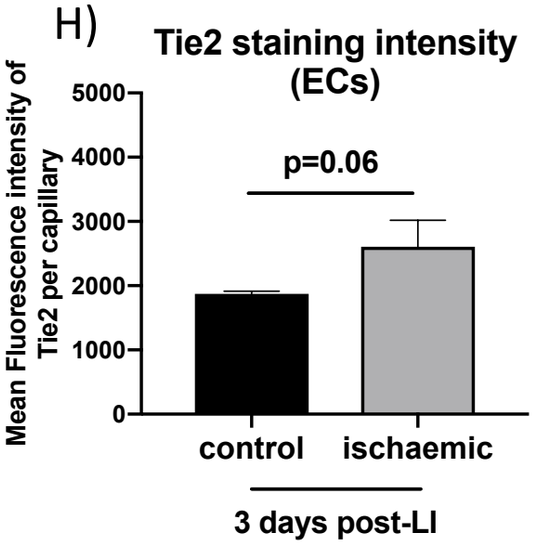

Supplementary figure S8

A)

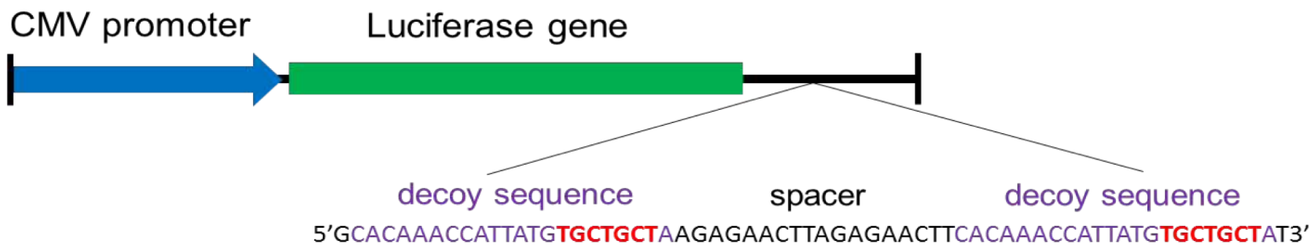

	"seed"
miR-15a	5'-UAGCAGCACAUAAUGGUUUGUG-3'
miR-16	5'-UAGCAGCACGUAAAUAUUGGCG-3'
miR-15b	5'-UAGCAGCACAUCAUGGUUUACA-3'
miR-503	5'-UAGCAGCGGGAACAGUUCUGCAG-3'

B)

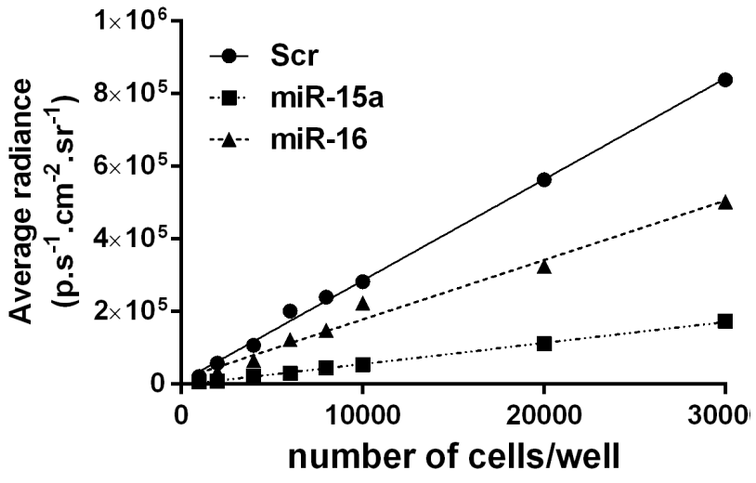

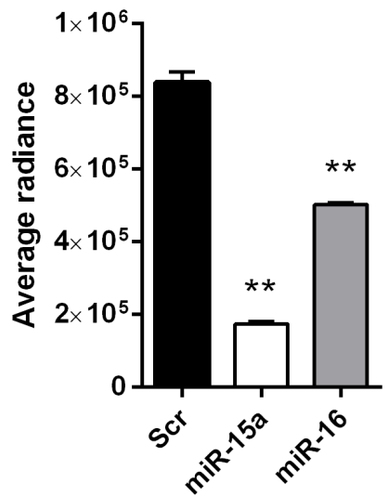

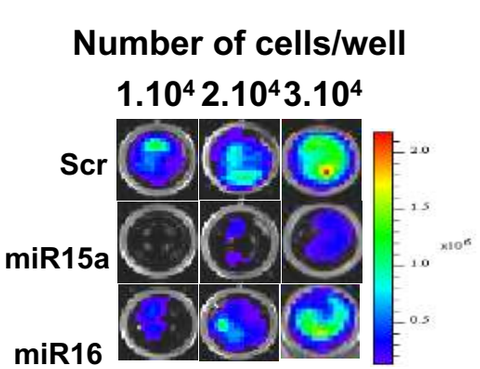

C)

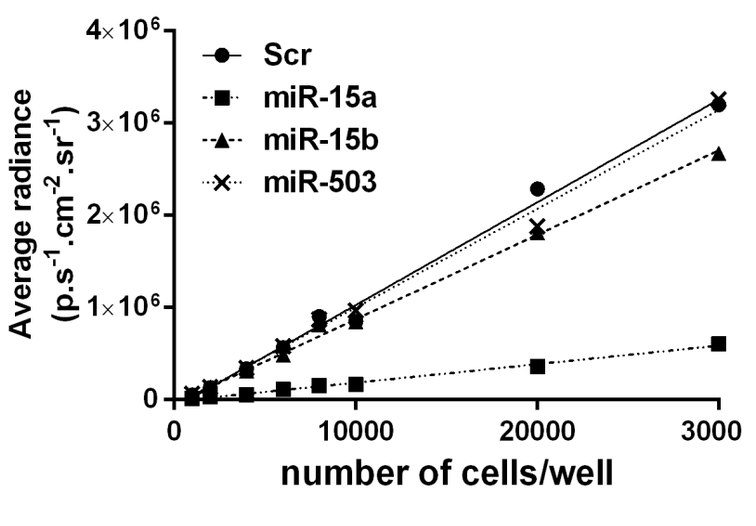

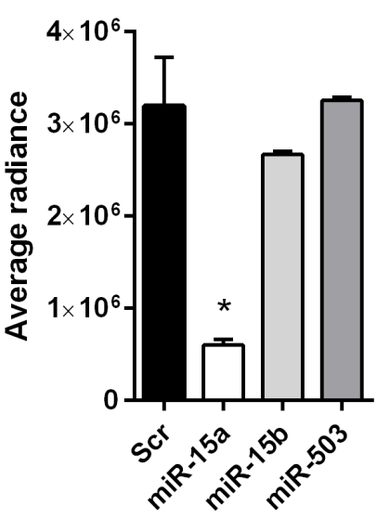

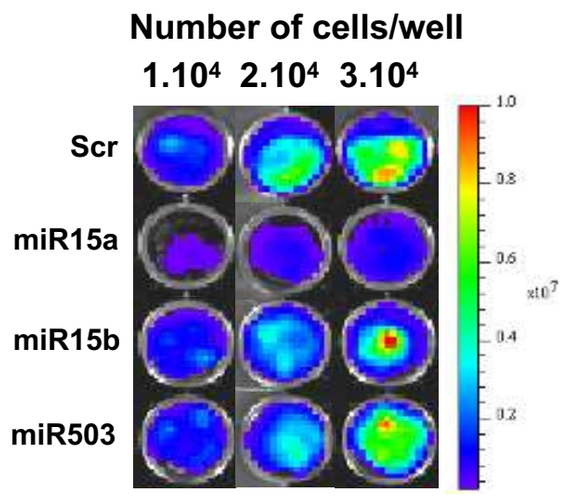

Supplementary figure S9

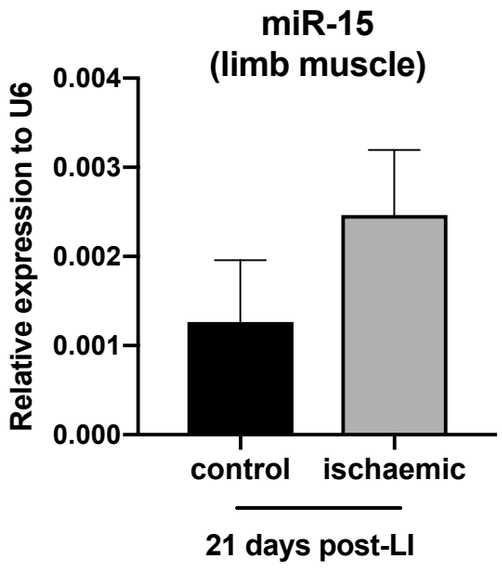

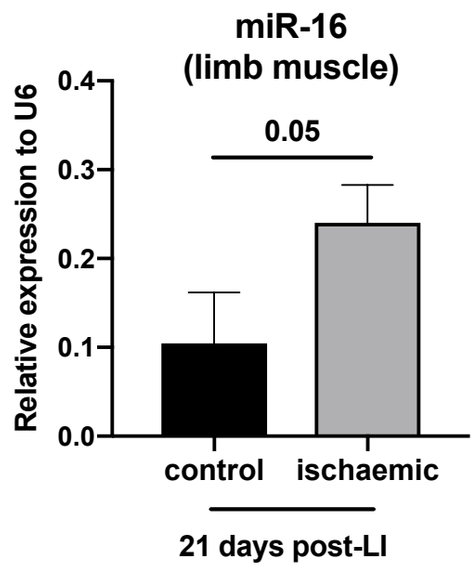

Supplementary figure S10

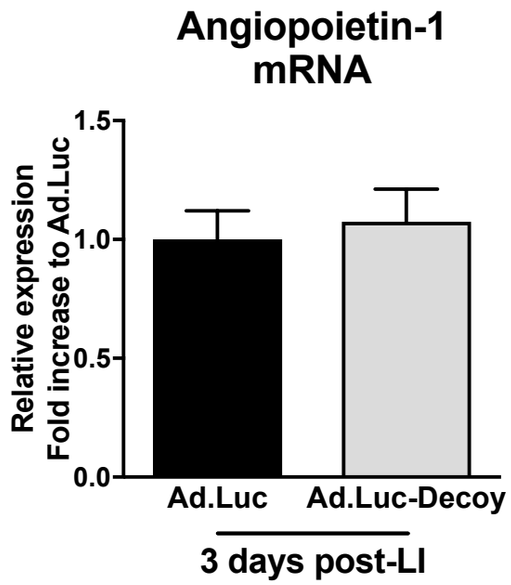

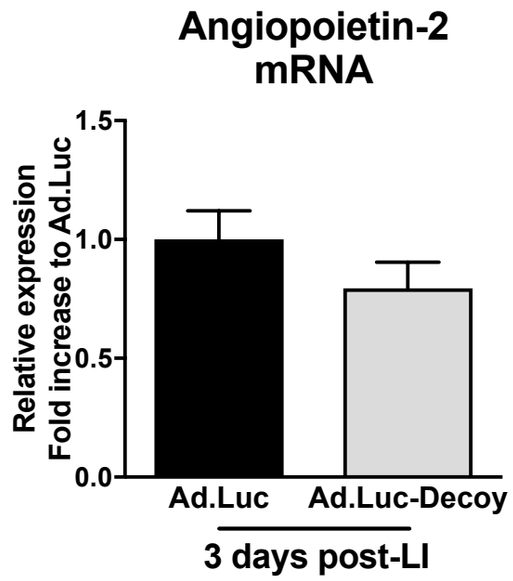

Supplementary figure S11

A)

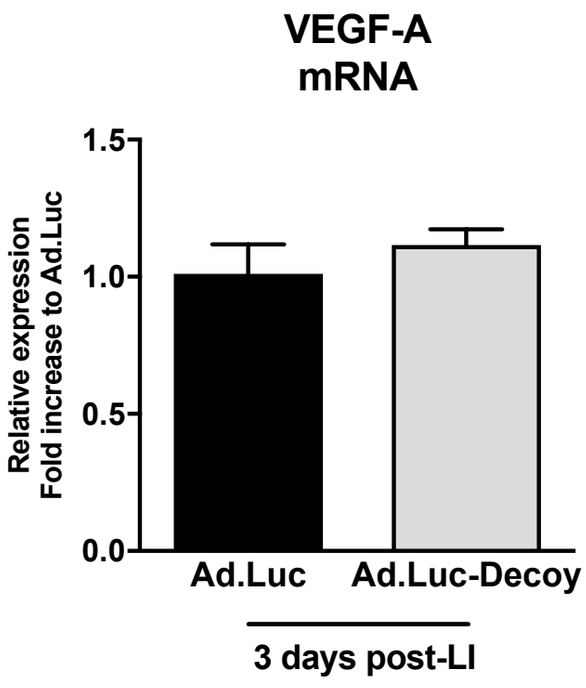

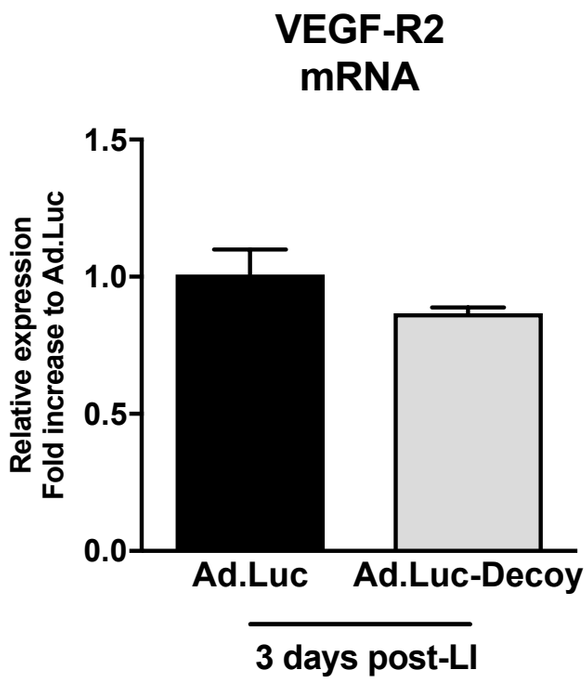

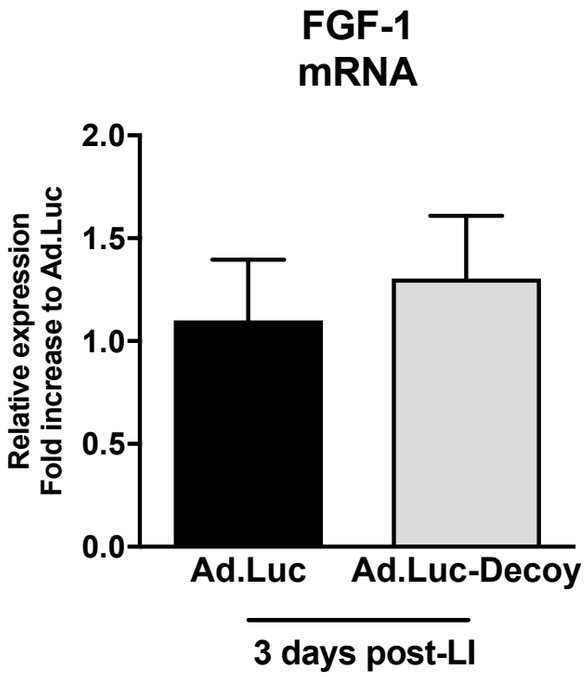

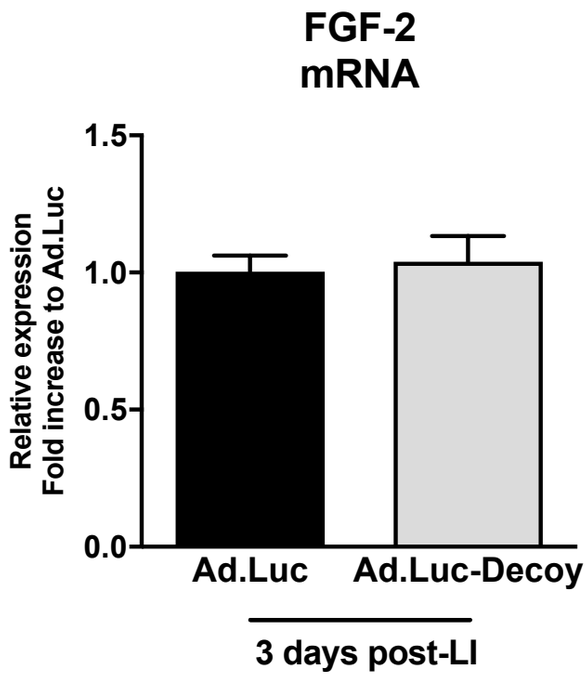

B)

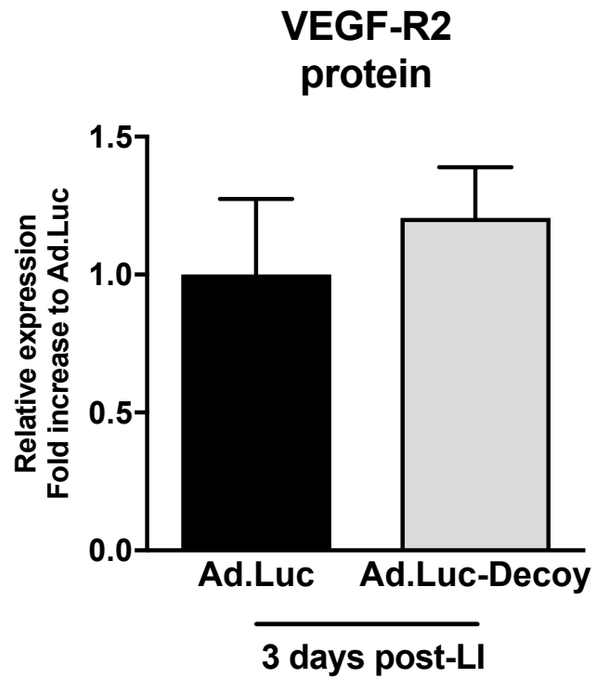

Supplemental data

Supplementary figure S1 : Expression of miR-16 and -210 in HUVECs is affected by hypoxia associated to serum deprivation, in opposition to miR-15a expression.

MiR-15a (A), -16 (B) and -210 (C) expressions were evaluated using RT-PCR in Human Umbilical Vein Endothelial Cells (HUVECs) cultured under normoxic and Foetal Bovine Serum (FBS)-complete (2% FBS) medium or hypoxic and FBS-free (0% FBS) medium for 24 or 48 h. Results were normalized to the small nuclear RNA U6 expression. Results are presented as mean ± SEM. n=3 per condition, *p < 0.05, **p < 0.01 and *** *p* < 0.001 *versus* time-matched normoxic and 2% FBS medium conditions.

Supplementary figure S2 : Expression of miR-15a and -16 in HUVECs is affected by serum deprivation but not by hypoxia, in contrast to hypoxamiR-210 expression.

MiR-15a, -16 and -210 expressions were evaluated using RT-PCR in Human Umbilical Vein Endothelial Cells (HUVECs) cultured under normoxic/hypoxic conditions (A-C), or Foetal Bovine Serum (FBS)-complete (2% FBS) or FBS-free (0% FBS) media (D-E) for 24 or 48 h. Results were normalized to the small nuclear RNA U6 expression. Results are presented as mean ± SEM. n=3-5 per condition, *p < 0.05 and **p < 0.01 *versus* time-matched normoxic or 2% FBS medium conditions.

Supplementary figure S3 : Increase of miR-15a and -16 in serum deprivation in HUVECs is due to an increase in precursor (pre-miR) maturation, and not an increase of primary transcript (pri-miR) transcription.

The mechanism behind the increased expression of miR-15a and -16 under serum deprivation was assessed in Human Umbilical Vein Endothelial Cells (HUVECs) cultured under Foetal Bovine Serum (FBS)-complete (2% FBS) or FBS-free (0% FBS) media for 24 or 48 h. (A) Expression of the primary transcript pri-miR-15a/-16-1 was measured by RT-PCR and normalized to Lamin B. (B, C, D) The relative expression of the precursors of miR-15a and -16 (pre-miR-15a/-16-1/-16-2) and the mature form of miR-15a (E) and -16 (F) was also measured by RT-PCR and normalized to small nuclear RNU6B. The relative expression of each mature miR compared to their precursors is also shown (G, H, I). Results are presented as mean ± SEM. n=3 per condition. *p < 0.05 , **p < 0.01 *versus* time-matched 2% FBS medium condition.

Supplementary figure S4 : MiR-15a and/or -16 inhibition decreases HUVEC tube formation on Matrigel assay.

Human Umbilical Vein Endothelial Cells HUVECs were transfected with a Scramble oligo (Scr) or an anti-miR against miR-15a or miR-16, or the two anti-miRs together (total concentration of 20 nM) to inhibit their activity. MiR-15a and miR-16 expression after anti-miR transfection in HUVECs was assessed using RT-PCR and normalized to small nuclear U6 (A). The angiogenic capacity of HUVECs (measured by network formation on Matrigel) after inhibition of miR-15a (B), miR-16 (C) and both miR-15a and -16 (D) was assessed and is presented as tube length (mm) per mm^2. Representative images of each condition are provided showing, in green, HUVECs stained with Calcein, 6 h after plating the cells on Matrigel. Scale bar: 100 µm. All experiments were performed in triplicate with n=3 per condition. All data are expressed as mean ± SEM. *p < 0.05 , **p < 0.01 vs. Scr-control.

Supplementary figure S5 : Bioinformatic analysis of potential targets of miR-15a and -16 involved in angiogenesis, positions of miR-15a and -16 seed sequence binding on the human sequence of *TEK* on chromosome 9, and validation of the target.

Predicted common targets of miR15/16 obtained from miRcode were subjected to gene ontology (GO) analysis using the program CLUEGO. (A) The top 15 significantly enriched GO terms are shown as a bar graph, with the x-axis indicating $-\log_2$ (p values) and significant GO terms on the y-axis. Higher values indicate greater statistical significance. An interesting term is "blood vessel development" that corresponds to 415 target genes. (B) miRcode results reveal that one of these 415 target genes is "*TEK*" which has a 6 bp binding site for miR15/16 in its coding sequence (shown in the UCSC browser highlighted in red) at position chr9: 27204938-27204943. At the bottom of the browser are Multiz alignments of 100 vertebrates, which indicate conservation as a grey-scale density plot, where darker regions indicate more conservation. (C) This predicted binding site of miR15/16 in the CDS region of *TEK* is most highly conserved in mammals (83%), followed by primates (67%) and vertebrates (46%).

Supplementary figure S6 : MiR-15a and -16 inhibition in HUVECs increases Tie2 expression level leading to an overall increase of Tie2 phosphorylation.

HUVECs were transfected with a Scramble oligo (Scr) or an anti-miR against miR-15a or miR-16, or the two anti-miRs simultaneously (total concentration of 50 nM) to inhibit their activity. Phospho-Tie2 (Y922) and total Tie2 protein expression were assessed by western blot and normalized to β-actin and expressed relatively to Scr condition. Results are presented as mean ± SEM. n=6 for each condition. Representative pictures of cropped WB images are also shown. * $p < 0.05$, ** $p < 0.01$ versus Scr condition.

Supplementary figure S7 : Tie2 and Angiopoietin(Ang)-1 and -2 expression in whole limb muscles and muscle-ECs in our model of limb ischemia.

Tie-2, Ang-1 and Ang-2 expression was evaluated by RT-PCR in control/non-ischemic limb muscles collected at 1 day (A) and 3 days (B) after limb ischemia (LI) induction. (C-H) Tie-2 expression in limb muscle ECs, identified by CD31 marker, was measured using immunohistofluorescence in limb muscle tissues, 1 day and 3 days after LI. (C&F) Representative microphotographs showing co-staining of Tie-2 (green) and CD31 (red) in contralateral (control) muscle and ischemic muscle (n=5 per group). Yellow arrows show Tie-2 positive capillaries (Tie-2+/CD31+) while white arrows show Tie-2 negative capillaries (Tie2-/CD31+). Scale bar: 50 µm. (E&F) The percentage of Tie-2+/CD31+ capillaries was analysed and the intensity of Tie-2 within the Tie-2+/CD31+ capillaries was also reported (G&H). n=4 per condition. Results were presented as mean ± SEM. ** $p < 0.01$, versus control condition.

Supplementary figure S8 : Adenovirus carrying a decoy sequence for miR-15a and -16 (*Ad.Luc-Decoy*), gene construction and inhibition efficiency *in vitro*.

(A) Schematic description of the functional decoy-miR15a/16 vector. The decoy sequence is perfectly complementary to the miR-15a sequence. CMV: cytomegalovirus immediate early promoter. Mature sequences of miR-15a, -15b, -16 and -503 are also provided. Efficiency of the virus has been evaluated in Hela cells infected with *Ad.Luc-Decoy* and transfected either with pre-miR scramble (Scr), pre-miR-15a (miR-15a) and pre-miR-16 (miR-16) at 25 nM (B) or with pre-miR-15b (miR-15b) and pre-miR-503 (miR-503) to investigate the specificity of the construct (C). (B and C) Results show the luciferase activity, measured on a Xenogen In Vivo Imaging System (IVIS), of increasing numbers of cells (1000-30000) plated in 96-well plates. Values obtained with 30000 cells and representative

images acquired with the IVIS system are also presented. Each well picture was cropped as cells were plated non-adjacently to avoid light-crossing between wells. Results are presented as mean ± SEM. Experiments were performed in duplicate, n=2 per condition, and expressed in as photons per second per centimetre-squared per steradian (p. s^{-1}. cm^{-2}.sr^{-1}). *p < 0.05 and **p < 0.01 *versus* the pre-miR Scr condition, Student's *t*-test.

Supplementary figure S9 : Mir-16 expression is increased 21 days after limb ischemia.

At 21 days after limb ischemia surgery, ischemic and non-ischemic/contralateral (control) adductor muscles were collected and the expression of miR-15a and -16 assessed by RT-PCR in the total muscle tissue. Results were normalized to snU6 (n=4-6). Results were expressed relatively to Ad.Luc control condition and presented as mean ± SEM.

Supplementary figure S10 : Inhibition of miR-15a/-16 in vivo does not modify the expression of Tie2 agonist Angiopoietin-1 and Angiopoietin-2 after limb ischemia.

Angiopoietin-1 and Angiopoietin-2 expression in ischemic adductor muscles, 3 days after limb ischemia surgery and injection with either Ad.Luc or Ad.Luc-Decoy virus, was assessed at mRNA level by RT-PCR. Results were normalized to 18S (n=6). Results were expressed relatively to Ad.Luc control condition and presented as mean ± SEM.

Supplementary figure S11 : Inhibition of miR-15a/-16 in vivo does not modify the expression of previously described targets of miR-15a and -16 in our model of limb ischemia.

(A) VEGF-A, VEGF-R2, FGFb, FGF-1 expression in ischemic adductor muscles, 3 days after limb ischemia surgery and injection with either Ad.Luc or Ad.Luc-Decoy virus, was assessed at mRNA level by RT-PCR. Results were normalized to GAPDH (n=3). (B) VEGF-R2 expression in ischemic adductor muscles, 3 days after limb ischemia surgery and injection with either Ad.Luc or Ad.Luc-Decoy virus, was assessed at protein level by western blot. Results were normalized to HSP-90 (n=6) and presented as mean ± SEM.

Supplementary Table 1: Information for probes used in TaqMan-based quantitative real-time PCR assays (Applied Biosystems, UK)

Gene ID	Reference
hsa/mmu-miR-15a	000389
hsa/mmu-miR-15b	000390
hsa/mmu-miR-16	000391
hsa/mmu-miR-503	001048
hsa/mmu-miR-210	000512
snRU6	001973

Supplementary Table 2: Information for primer-pairs used in SYBR Green-based quantitative real-time PCR assays (Sigma and Qiagen)

Gene ID	SEQUENCE
human pri-miR-15a-16-1	forward: 5’-AAGGTGCAGGCCATATTGTG-3’
	reverse: 5’-AAGGCACTGCTGACATTGC-3’
human β-actin	forward: 5’-TGGACATCCGCAAAGACCTGT-3’
	reverse: 5’-GGGCAGTGATCTCCTTCTGCA-3’
human GAPDH	forward: 5’-TGCACCACCAACTGCTTAGC-3’
	reverse: 5’-GGCATGGACTGTGGTCATGAG-3'
human LaminB	forward: 5’-CTGGAAATGTTTGCATCGAAGA-3’
	reverse: 5’-GCCTCCCATTGGTTGATCC-3'
human Tie2	forward: 5’-GGGACCCCACACTTCCAACAA-3’
	reverse: 5’-TTTGGTATCAGCAGGGCTGG-3'
human/mouse 18S	forward: 5’-CCCAGTAAGTGCGGGTCATAA-3'
	reverse: 5’-CCGAGGGCCTCACTAAACC-3'
mouse angiopoietin1	forward: 5’-GGGGGAGGTTGGACAGTAA-3’
	reverse: 5'-CATCAGCTCAATCCTCAGC-3'
mouse angiopoietin2	forward: 5’-GATCTTCCTCCAGCCCCTAC-3’
	reverse: 5'-TTTGTGCTGCTGTCTGGTTC-3'
mouse FGF-1	forward: 5’-AAAGTGCGGGCGAAGTGTA-3’
	reverse: 5'-CTCATTTGGTGTCTGCGAGC-3'
mouse FGFb	forward: 5’-GGCTGCTGGCTTCTAAGTGT-3’
	reverse: 5'-GTCCCGTTTTGGATCCGAGT-3'
mouse VEGF-A	forward: 5’-GGAGATCCTTCGAGGAGCACTT-3’
	reverse: 5'-GGCGATTTAGCAGCAGATATAAGAA-3'
mouse VEGF-R2	forward: 5’-TACAGACCCGGCCAAACAA-3’
	reverse: 5'-TTTCCCCCCTGGAAATCCT-3'
mouse Tie2	forward: 5’-TACAACGGCCATTTCTCCTC-3’
	reverse: 5’-GTGGCTTGCTTGGTACAGGT-3'
miR-15a	forward: 5'-TAGCAGCACATAATGGTTTGTGAAA-3'
miR-16	forward: 5'-TAGCAGCACGTAAATATTGGCGAA-3'
pre-miR-15a	forward : 5'-GCACATAATGGTTTGTGGATTT-3'
pre-miR-16-1	forward : 5'-GTAAATATTGGCGTTAAGATTC-3'
pre-miR-16-2	forward : 5'-GCGTAGTGAAATATATATTAAACACC-3'